Modifying the adsorption characteristic of inert silica films by inserting anchoring sites

Stefan Ulrich, Niklas Nilius*, Hans-Joachim Freund
Fritz-Haber-Institut der MPG
Berlin, Germany

Umberto Martinez, Livia Giordano, Gianfranco Pacchioni*
Dipartimento di Scienza dei Materiali, Università di Milano-Bicocca,
Via R. Cozzi, 53 – 20125, Milano, Italy

The adsorption properties of silica thin films on Mo(112) have been tailored by embedding single Pd atoms into the nano-pores of the oxide material. The embedded Pd is able to anchor metal adatoms that would not bind to the inert silica surface otherwise. Several adsorption structures, e.g. Pd-Pd, Ag-Pd and Au-Pd complexes, have been prepared in this way and analyzed with STM and DFT. The binding strength of the different adatoms to the surface is determined by the number of electrons in their frontier orbitals, which introduce a repulsive interaction with the oxide electronic states and weaken the covalent bond to the Pd anchor.

PACS: 68.43.Fg (Adsorbate structure), 68.47.Gh (Oxide surfaces),
68.37.Ef (Scanning tunneling microscopy) 71.15.Mb (Density functional theory)

*Corresponding Aauthors: nilius@fhi-berlin.mpg.de, gianfranoc.pacchioni@unimib.it

Tailoring the adsorption properties of solid materials has been a long-term perspective in surface science.[1,2,3] The functionalization of surfaces combines several aspects. First, the density and spatial arrangement of surface binding sites needs to be determined. Second, the adsorption should be chemically sensitive; admitting only selected species to interact with the surface. And last, the internal structure of the ad-material should be controllable. Surfaces with such designable adsorption properties have a wide range of applications, for instance to catalyze stereo-selective reactions, to produce chemical sensors, and to prepare regular adsorption patterns for electronic and magnetic devices.[4]

Several approaches have been made to fabricate tunable adsorption systems; however, most of them are unable to fulfill all of the above-given specifications. Regular arrays of binding sites are produced on vicinal surfaces,[5] molecular template structures,[6] and epitaxial systems exhibiting an ordered network of dislocations.[7,8] Chemical sensitivity is achieved by equipping the surface with suitable functional groups to stimulate interconnection with the desired adsorbates. Alternatively, the size-selective adsorption characteristic of porous materials, e.g. zeolites, is exploited to tune surface reactions via the size of the adsorbates.[1,9] The control of the internal structure of the ad-material remains the most difficult part. Here, mainly atomic manipulation with the scanning tunneling microscope (STM) have been employed to assemble surface aggregates with a defined structure and chemical composition.[10,11]

In this paper, a new approach towards a functionalized adsorption system is presented that is based on the introduction of defined binding sites into an originally inert surface. A suitable system for experimental realization is the porous silica film that can be gown on Mo(112).[12,13] The film is chemically inert and only physisorbs inorganic molecules like CO and H_2O.[14] However, single metal atoms can be inserted into the oxide nano-pores[15], as demonstrated for Pd and Ag.[16,17] Gold atoms, on the other hand, are unable to penetrate the silica pores due to their larger diameter with respect to the pore size.[18] After insertion, the metal atoms remain close to the surface and might be used to stabilize adsorbates to the otherwise non-reactive oxide film.

The approach is comparable to the doping of oxide materials with impurity atoms or point defects, as another means to create new binding sites. Substantial changes in the adsorption behavior were indeed reported for Li- or Ti-doped SiO_2, and MgO surfaces

containing oxygen vacancies.[15,19,20,21,22] However, while doping affects the global electronic and chemical properties of the oxide material, embedding of suitable single-atom anchors modifies the binding characteristic only locally.

This paper reports on the fabrication of a functionalized silica film via the incorporation of a defined number of Pd atoms into its top-layer. These anchor sites are able to stabilize single adatoms on the oxide surface, as revealed from the combined STM and density functional theory (DFT) study. The silica film modified in this way fulfills several requirements of a functionalized adsorption system, as the density, chemical nature and binding geometry of adsorbates can be controlled.

The experiments are performed in a costume built UHV-STM operated at 10 K. The silica film is prepared on an oxygen pre-covered Mo(112) surface by depositing 1.2 ML silicon at 800 K in an oxygen ambience of 1×10^{-7} mbar.[12,13] Sample annealing to 1200 K leads to the formation of a crystalline SiO_2 layer, as indicated by the sharp c(2x2) LEED pattern.[13] The film is composed of a network of corner-sharing SiO_4 tetrahedrons, whereby every Si is connected via bridging oxygen atoms to three neighboring Si in the plane and to the Mo surface underneath (Fig.1A, inset). The resulting honeycomb structure consists of -Si-O- hexagons enclosing a hole of 3-4 Å diameter that gives access to a nano-pore at the Mo-SiO_2 interface. The main structural defects of the film are domain boundaries along the $[\bar{1}10]$ direction, caused by the lateral displacement of two oxide patches by one $[\bar{1}\bar{1}1]$-oriented Mo unit cell vector (Fig.2, dashed arrows). Along such boundaries, the regular hexagons are replaced by larger -Si-O- octagons alternating with -Si-O- squares.

Single metal atoms are deposited onto the film from high-purity metal wires (99.95%) wrapped with a tungsten filament. Although deposition is performed at 20 K sample temperature, the atoms have sufficient initial energy to perform transient diffusion into their equilibrium configuration. The electronic properties of the sample surface are probed by differential conductance (dI/dV) spectroscopy performed with lock-in technique and open feed-back loop (10-15 mV modulation bias, 1137 Hz).

DFT calculations are carried out with the generalized gradient approximation using the PW91 exchange-correlation functional and a plane wave basis set (kinetic energy cut-off 400 eV) as implemented in the VASP code.[23,24,25] The electron-ion

interaction is described by the projector augmented wave method (PAW) developed by Blöchl.[26] The Mo(112) substrate is modeled by seven Mo layers separated by a vacuum slab of at least 10 Å. The three bottom Mo layers are kept frozen at bulk positions during geometry optimization. A (4×2) and a (6×4) super-cell are used to describe the silica film, which corresponds to a sample stoichiometry of $Mo_{14}Si_2O_5$ and $Mo_{24}Si_6O_{15}$, respectively.

STM topographic images of the bare oxide film show the characteristic honeycomb structure of the silica. Upon Pd exposure, distinct hexagonal stars appear in the images taken at 0.5 V (Fig. 1A). They transform into bright protrusions of approximately 0.7 Å height above 2.0 V imaging bias. According to earlier studies[18], the features are assigned to Pd atoms that have penetrated the silica nano-pores and bind to the Mo-SiO_2 interface with roughly 3.3 eV (referred to as Pd_{sub}). The characteristic star-like contrast originates from hybridization between the *O 2p* and the *Pd 5s* orbitals, which renders the oxygen atoms of the hosting -Si-O- hexagon visible in the STM. Above +2.0 V sample bias, the *Pd 5s* becomes directly accessible for tunneling electrons and the contrast localizes at the Pd_{sub} atom in the center of the hexagon.[18] In the following, the possibility to anchor single atoms to these Pd_{sub} species shall be investigated.

For this purpose, three sets of experiments are performed: (i) deposition of 1×10^{13} Pd atoms per cm^2 onto SiO_2/Mo(112) pre-covered with 2×10^{13} cm^{-2} Pd_{sub}, (ii) deposition of 1×10^{12} cm^{-2} Au atoms and (iii) 1×10^{12} cm^{-2} Ag atoms onto a silica film that already contains 1×10^{13} cm^{-2} Pd_{sub} (Fig.1B-D). In all three cases, new species appear on the oxide surface that clearly differ in apparent height, shape and bias-dependent contrast from the Pd_{sub} anchors. The species are imaged as round protrusions at all sample bias, in contrast to the distinct hexagonal shape of inserted Pd_{sub}, and reach apparent heights of more than 2.0 Å (compared to 0.7 Å for Pd_{sub} at optimum imaging conditions). They are not compatible with single Ag or Au atoms on the silica surface, either. According to DFT calculations, both atomic species only weakly interact with the oxide film (adsorption energies below 0.05 eV) and perform rapid diffusion even at low temperature.[15,18] Whereas the Ag atom is able to pass the opening in the -Si-O- hexagons with finite probability, producing similar features in the STM as the Pd_{sub}, the Au atom is too big for penetration and binds exclusively at domain boundaries exposing larger pores. As the

new species are neither located along domain boundaries nor exhibit the unusual contrast of an embedded atom, they can safely be discriminated from Ag and Au monomers. The adsorption structures emerging after Pd, Ag or Au deposition onto a Pd_{sub}-covered SiO_2 film are therefore assigned to single adatoms bound to Pd_{sub} anchors in the silica; a hypothesis that will be supported by further experimental evidence in the following.

The new ad-species are easily altered with a moderate voltage pulse applied to the STM tip (3-5V) that removes the top atom, as demonstrated for a Pd-Pd_{sub} complex in Fig.2. After the manipulation experiment, the characteristic signature of an embedded Pd_{sub} becomes visible in every case, suggesting that a Pd_{sub} anchor is indeed required to stabilize the complex. Furthermore, the different ad-structures exhibit characteristic dI/dV fingerprints, which clearly differ from the spectroscopic response of the monomer species. For instance, while a Pd_{sub} shows a weak dI/dV shoulder at +2.3 V sample bias, attributed to the *Pd 5s* orbital,[18] a pronounced maximum at +1.75 V is observed for the Pd-Pd_{sub} complex (Fig. 3A). Similarly, the Au-Pd_{sub} species shows enhanced intensity in dI/dV maps taken at -0.2 V and +1.6 V (Fig.4), whereas no maxima are revealed for Au monomers attached to the domain boundaries. Only for Ag-Pd_{sub} species, no dI/dV spectra could be acquired, because the Ag atom easily desorbs from the surface during a spectroscopic run.

The attachment of Pd, Ag, and Au atoms to Pd_{sub} anchors in the silica film is verified by DFT calculations. In all three examples, the adatoms form covalent bonds with a Pd_{sub} sitting in an oxide nano-pore; however, binding energies and metal-metal bond lengths are rather different. The strongest interaction is found for Pd atoms, which bind with 1.16 eV to the Pd_{sub} (bond length: 2.66 Å). Without surface anchor, the adatom only interacts with 0.35 eV to an oxygen atom, but would in fact penetrate the opening in the -Si-O- hexagon. Binding energies are considerably smaller for noble-metal adatoms and have been calculated with 0.35 eV for Au-Pd_{sub} and 0.19 eV for Ag-Pd_{sub} complexes (virtually no binding without Pd_{sub}). Surprisingly, the atom-atom bond lengths are with 2.54 Å for Au-Pd_{sub} and 2.85 Å for Ag-Pd_{sub} species not much different from the Pd-Pd_{sub} case. Furthermore, the inter-atomic distances of the surface complexes are close to the values of the corresponding gas-phase dimers (Pd_2: 2.54 Å, Au-Pd: 2.68 Å), although the interaction energies follow a different trend (gas phase Pd_2: 0.7 eV, Au-Pd: 1.4 eV).[27,28]

This apparent contradiction between the short inter-atomic distances and the low binding energies of the different adsorption complexes indicates the presence of two competing interaction mechanisms on the silica surface. On the one hand, the adatoms form strong covalent bonds to the Pd_{sub} anchors. This attractive contribution is, however, counterbalanced by a Pauli repulsion between the adatom orbitals and the *O 2p* states of the surface oxygen atoms, to which the Si electronic states only weakly contribute. The repulsive term is dominated by the spatially most expanded orbital of the respective adatom, which is the *5s* for the Pd and Ag atom and the *6s* for the Au. Those frontier orbitals hybridize with the *O 2p* states upon adsorption and form new states of anti-bonding character that weaken the adatom-surface interaction (Fig. 3B). The strength of the repulsion is given by the number of electrons in these hybrid states. The *O2p-Pd5s* state is located at +1.25 eV above the Fermi level and therefore empty, which reduces the repulsion of the surface oxygen atoms and allows the formation of a strong Pd-Pd_{sub} bond. The interaction energy is even higher than in gas-phase Pd_2, reflecting the stabilization effect of the Mo-support below the silica film. The unoccupied nature of the hybrid state manifests the charge neutrality of the surface-bound Pd atom, as the *5s* orbital is empty in a gas-phase species, too. The presence of an empty *O2p-Pd5s* resonance state is also compatible with the dI/dV peak at +1.75 V observed in the conductance spectrum of the Pd-Pd_{sub} complex (Fig. 3A).

In contrast, the hybrid state formed between the *Ag 5s* (*Au 6s*) orbital and the surface *O 2p* states is singly (doubly) occupied, as deduced from its calculated energy position at +0.1 eV (-0.3 eV) (Fig. 3B). The electron(s) in these anti-bonding states induce substantial Pauli repulsion with the silica LDOS, which partly compensates the attractive interaction with the Pd_{sub} and gives rise to the small binding energies of the Ag-Pd_{sub} and Au-Pd_{sub} complexes. In both cases, the hybrid states could not be identified in dI/dV spectroscopy, most likely due to their position close to the Fermi level. Only the small intensity increase in dI/dV maps of the Au-Pd_{sub} species taken at -0.2 V might provide an experimental evidence for the presence of the occupied *O 2p-Au 6s* state (Fig. 4). The complete filling of the Au *6s*-derived state also indicates a negative charging of the Au adatom, since the gas phase Au is in a $6s^1$ configuration. The extra electron is transferred from the Mo support into the *Au 6s* orbital as it shifts below the Fermi level

upon adsorption. A similar charging behavior has been observed for Au atoms on other oxide films before.[29,30] The Ag adatom, on the other hand, remains neutral on the silica surface, since the *Ag 5s* is singly occupied in both, the surface and the gas-phase species.

To reduce steric repulsion, the -Si-O- hexagon hosting the Pd_{sub} strongly relaxes when forming the bond to the different adatoms. The effect is most pronounced for the Au-Pd_{sub} complex due to the diffuse nature and the double occupancy of the *Au 6s* orbital. According to the DFT calculations, the opening in the -Si-O- hexagon increases by several tenths of an Angstrom (~5%) to allocate more space for the Au atom. As a result, the Au binding energy to the Pd_{sub} increases by roughly a factor of two upon relaxation (0.35 eV as calculated with a 6×4 unit cell that permits relaxation versus 0.14 eV without relaxation). The ring widening is accompanied with a local reduction of the silica LDOS around the Au-Pd_{sub} binding site, which originates from the decreasing Si-O orbital overlap in the enlarged hexagon. The reduced state density can indeed be observed in conductance maps of the Au-Pd_{sub} complex taken in a bias range between 1.0 and 1.5 V (Fig. 4). To balance the outward relaxation of the hexagon, Si-O bonds need to be compressed in a circular region surrounding the adsorption site. The resulting increase of the oxide LDOS becomes also visible in the dI/dV maps, and shows up as a ring-like intensity enhancement in the vicinity of the Au-Pd_{sub} species The ring diameter is approximated with 10 Å, indicating that mainly the next shell of -Si-O- hexagons is affected by the compressive stress exerted by the enlarged silica pore. Similar ring structures are also observed in the dI/dV maps of Pd-Pd_{sub} complexes (not shown).

In conclusion, the possibility to prepare defined Pd-Pd_{sub}, Au-Pd_{sub} and Ag-Pd_{sub} complexes on a thin silica film has been demonstrated by STM and DFT. The ad-structures consist of a Pd_{sub} atom inserted into a nano-pore of the silica host, which stabilizes the different adatoms via strong covalent bonding. This attractive interaction is partly compensated by the Pauli repulsion exerted by the *O 2p* states of the surface oxygen atoms. The repulsive contribution is governed by the electron occupancy of the frontier orbitals of the adatoms and increases when going from the Pd ($5s^0$ configuration) to the Ag ($5s^1$) and Au ($6s^2$) ad-species. The binding strength to the Pd_{sub} anchor therefore depends on the nature of the adsorbate, giving rise to a certain chemical sensitivity of the interaction mechanism. The approach taken here can in principle be extended to the

fabrication of complex surface aggregates, whereby the different atomic species are subsequently attached to the surface anchor. The successful insertion of single-atom binding sites into a porous SiO_2 film on Mo(112) therefore presents a first step towards a functionalized adsorption system.

Acknowledgements

The work has been supported by the COST Action D41 “Inorganic oxides: surfaces and interfaces”. Part of the computing time was provided by the Barcelona Supercomputing Center (BSC-CNS).

Figure Captions

Fig. 1

(A) STM topographic image of SiO_2/Mo(112) after insertion of Pd_{sub} species (U_s = 1.2 V, 14 × 14 nm^2). **(B)** Same surface after additional deposition of single Pd (0.5 V) **(C)** Au (0.5 V) and **(D)** Ag atoms (1.9 V, 14 × 14 nm^2). While only Pd_{sub} species are observed in (A), new ad-structures become visible in (B-D). The inset in (A) shows a structure model of a Pd_{sub} inserted into a silica pore (yellow circles: Si, red: O, pale-blue: Mo).

Fig. 2

(A) STM topographic image of Pd_{sub} and Pd-Pd_{sub} species on SiO_2/Mo(112) (U_s = 1.0 V, 10 × 10 nm^2). **(B)** As in (A) but after controlled removal of the adatom marked by the square box. **(C)** As in (B) but with enhanced contrast to show the silica atomic structure. Below the removed atom, the characteristic signature of an embedded Pd_{sub} becomes visible that has initially anchored the ad-species. The circles indicate other Pd-Pd_{sub} complexes as guides for the eye; the dashed arrows mark a domain boundary in the silica film.

Fig. 3

(A) dI/dV spectra of a Pd_{sub}, a Pd-Pd_{sub} complex and the bare silica film on Mo(112) (setpoint 2.5 V, 0.1 nA) . **(B)** Calculated LDOS of the bare silica film (dashed region). The line spectra depict the *Pd 5s*, (solid line), *Ag 5s* (dash-solid line) and *Au 6s* (dashed line) contribution to the hybrid state formed with the *O 2p* orbitals, when the respective adatom binds to a Pd_{sub} anchor. The calculated *Pd 5s*-resonance corresponds to the dI/dV peak observed for the Pd-Pd_{sub} complex in (A).

Fig. 4

Topographic image and dI/dV maps of a Pd_{sub} and an Au-Pd_{sub} species on silica/Mo(112) taken as a function of sample bias (6 × 6 nm^2). The increase of the dI/dV signal at the Au-Pd_{sub} position at -0.2 and +1.55 V marks intrinsic electronic states of the complex, while the ring-like enhancement visible between 1.0-1.5 V is related to a structural deformation of the silica lattice upon Au adsorption.

[1] H. Li, M. Eddaoudi, M. O'Keeffe, O. M. Yaghi, Nature **402,** 276 (1999).
[2] C. S. R. Kumar [Ed.], *Functionalization of nanomaterials*, (Wiley-VCH, Weinheim, 2005).
[3] H. J. Freund, Surf. Sci. **601,** 1438 (2007).
[4] N. Miyaura, A. Suzuki, Chem. Rev. **95**, 2457 (1995).
[5] N. Neel, J. Kröger, R. Berndt, Appl. Phys. Lett. **88**, 163101 (2006).
[6] J. A. Theobald, N. S. Oxtoby, M. A. Phillips, N. R. Champness, P. H. Beton, Nature **424**, 1029 (2003).
[7] H. Brune, M. Giovannini, K. Bromann, K. Kern, Nature **394**, 451 (1998).
[8] C. Becker, A. Rosenhahn, A. Wiltner, K. von Bergmann, J. Schneider, P. Pervan, M. Milun, M. Kralj, and K. Wandelt, New J. Phys. **4**, 75 (2002).
[9] S. Bhatia, *Zeolite catalysis: principles and applications*, (Boca Raton, 1990, CRC Press).
[10] N. Nilius, T. M. Wallis, and W. Ho, Science **297**, 1853 (2002).
[11] G. V. Nazin, X. H. Qui, W. Ho, Science **302**, 77 (2003).
[12] T. Schroeder, M. Adelt, B. Richter, M. Naschitzki, M. Bäumer, H.-J. Freund, Surf. Rev. & Lett. **7**, 7 (2000).
[13] J. Weissenrieder, S. Kaya, J.L. Lu, H. Gao, S. Shaikhutdinov, H.-J. Freund, M. Sierka, T. K. Todorova, J. Sauer, J. Phys. Rev. Lett. **95**, 076103 (2005).
[14] J. B. Giorgi, T. Schröder, M. Bäumer, H.-J. Freund, Surf. Sci. Lett. **498**, L71 (2002).
[15] L. Giordano, A. Del Vitto, G. Pacchioni, J. Chem. Phys. **124**, 034701 (2006).
[16] M. Baron, D. Stacchiola, S. Ulrich, N. Nilius, S. Shaikhutdinov, H.-J. Freund, U. Martinez, L.Giordano, G. Pacchioni, Chem. Phys. C. **112,** 3405 (2008).
[17] S. Ulrich, N. Nilius, H-J. Freund, U. Martinez, L. Giordano, G. Pacchioni, submitted.
[18] S. Ulrich, N. Nilius, H-J. Freund, U. Martinez, L. Giordano, G. Pacchioni, ChemPhysChem. **9**, 1367 (2008).
[19] J. X. Wang, J. H. Lunsford, J. Phys. Chem. **90**, 5883 (1986).
[20] M. C. Wu, C. M. Truong, D. W. Goodman, Phys. Rev. B **46**, 12688 (1992).
[21] B. K. Min, W. T. Wallace, D. W. Goodman, J. Chem. Phys. B **108**, 14609 (2004).
[22] M. Sterrer, M. Yulikov, E. Fischbach, M. Heyde, H.-P. Rust, N. Nilius, G. Pacchioni, T. Risse, H.-J. Freund, Angew. Chem. Int. Ed. **45**, 2630 (2006).
[23] J. P. Perdew, J. A. Chevary, S. H. Vosko, K. A. Jackson, M. R. Pederson, D. J. Singh, C. Fiolhais, Phys. Rev. B **46**, 6671 (1992).
[24] G. Kresse, J. Hafner, Phys. Rev. B **47**, 558 (1993).
[25] G. Kresse, J. Furthmüller, Phys. Rev. B **54**, 11169 (1996).
[26] P. E. Blöchl, Phys. Rev. B **50**, 17953 (1994).
[27] D. Andrea, U. Haussermann, M. Dolg, H. Stoll, H. Preuss, Theor. Chim. Acta 78 (1991) 247; P. Schwerdtfeger, Chem. Phys. Lett. **183,** 457 (1991); J. Ho, K. M. Ervin, M. L. Polak, M. K. Gilles, W. C. Lineberger, J. Chem. Phys. **95**, 4845 (1991).
[28] A. M. Joshi, W. N. Delgass, K. T. Thomson, J. Phys. Chem. B, **110,** 16439 (2006); D.R. Lide (Ed.), *Handbook of Chemistry and Physics*, (CRC Press, Boca Raton, Florida, 1998).
[29] M. Sterrer, T. Risse, U. Martinez Pozzoni, L. Giordano, M. Heyde, H.-P. Rust, G. Pacchioni, H.-J. Freund, Phys. Rev. Lett. **98**, 096107 (2007).
[30] N. Nilius, M. V. Ganduglia-Pirovano, V. Brázdová, M. Kulawik, J. Sauer, H.-J. Freund, Phys. Rev. Lett. **100**, 096802 (2008).

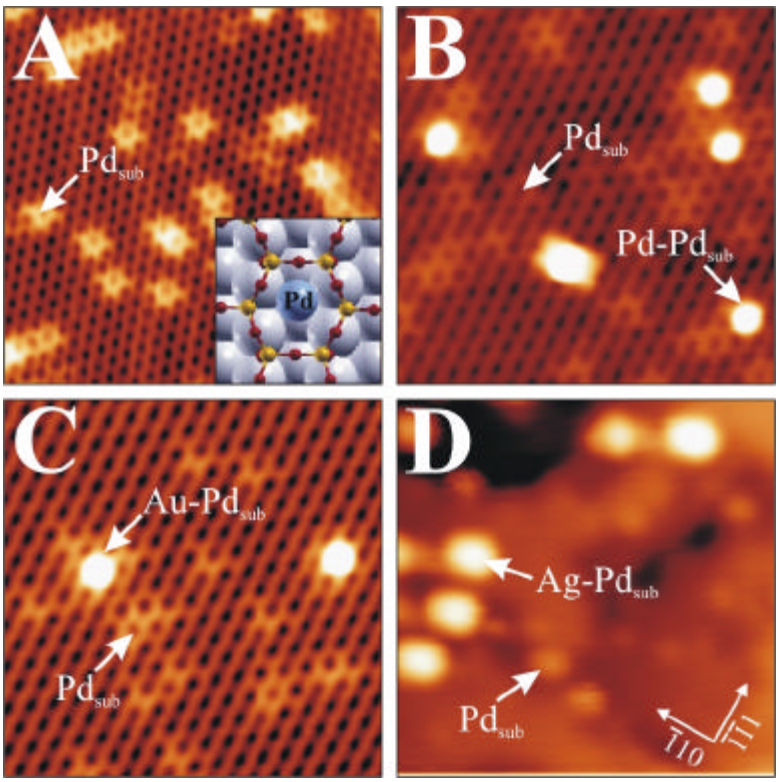

Figure 1

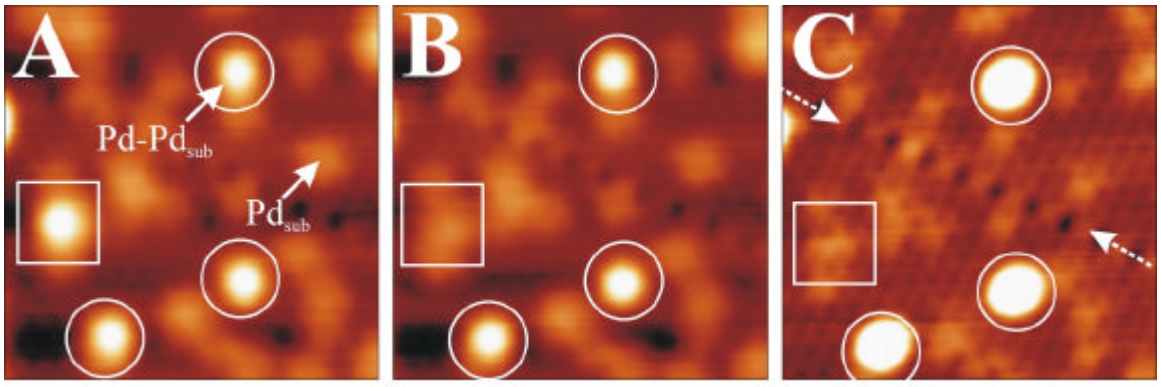

Figure 2

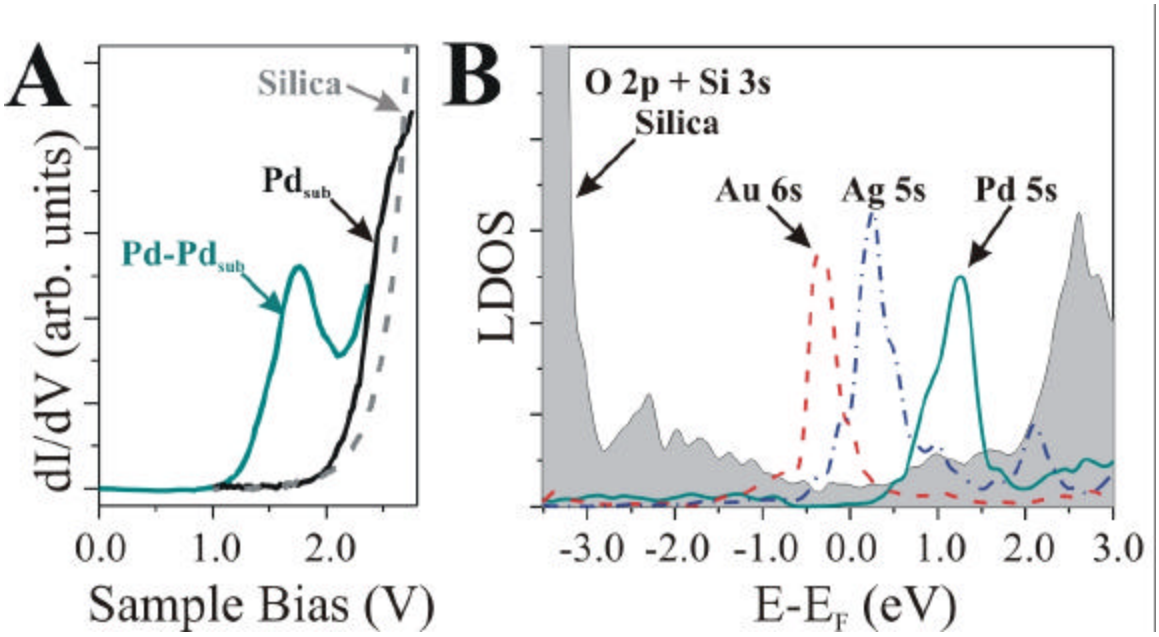

Figure 3

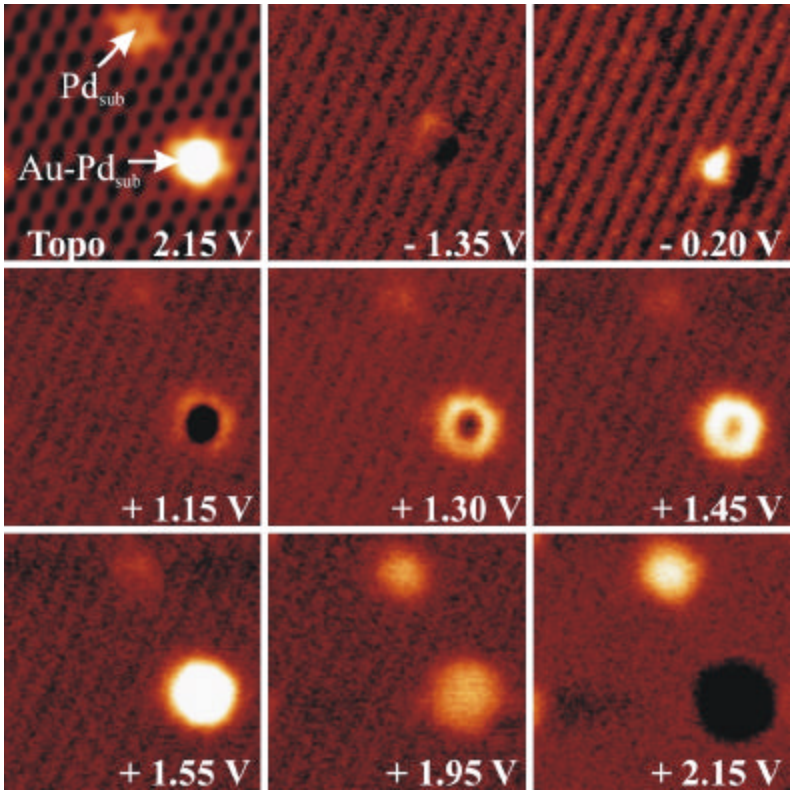

Figure 4